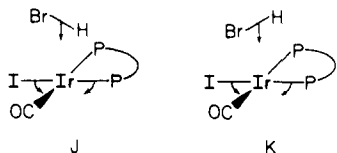


pathway ii, clearly indicates that the ease of trans ligand deformation or bending in $\text{IrX}(\text{CO})(\text{dppe})$ without regard to incoming substrate cannot by itself account for the stereoselectivity of these oxidative addition reactions. Thus, the complex-substrate interaction must be substantially different for HX vs. H_2 and R_3SiH . The first question that must be addressed is whether the HX addition is concerted or proceeds in two or more discrete steps. The stereoselective nature of the reaction where H and X ligands occupy cis positions in the kinetic product strongly suggests a concerted mechanism. In such a mechanism, the approach of the highly polar species HX along the P-Ir-I axis of $\text{IrI}(\text{CO})(\text{dppe})$ will undoubtedly be unsymmetrical and can be either electrophilic or nucleophilic in character as shown in **J** and **K**, respectively.



If HBr approach is nucleophilic as in **K** the situation resembles that of silane approach H and similar considerations would apply regarding the diastereoselectivity. Thus, the developing trigonal bipyramid of $\text{IrI}(\text{CO})(\text{dppe}) + \text{HBr}$ would be more stable with the better π -acid CO in the equatorial plane than with iodide there, and the concerted addition of HBr would be expected to proceed along P-Ir-CO , pathway i. This expectation is contrary to what is observed.

For electrophilic approach **J**, the bending of P-Ir-I leads to a complex + substrate trigonal bipyramid having the better donor iodide in the equatorial plane thus enhancing the ability of $\text{Ir}(\text{I})$

to donate electrons to an incoming electrophile. It is well established that $\text{Ir}(\text{I})$ complexes can act as electron pair donors as in the reactions of $\text{IrCl}(\text{CO})(\text{PPh}_3)_2$ with BF_3 and NO^+ and the oxidative addition reaction of MeI . In the present case, the donor ability of the Ir complex is better if P-Ir-X bends than if P-Ir-CO bends, and this leads to the observed diastereoselectivity. The primary interaction of hydrogen halides with $\text{IrX}(\text{CO})(\text{dppe})$ in nonpolar media, while leading to concerted addition, clearly differs from that of H_2 and R_3SiH . We conclude that in concerted oxidative addition reactions to cis phosphine analogues of Vaska's complex, the stereochemistry of addition (i.e., pathway i or ii) can be controlled kinetically by the nucleophilic or electrophilic character of the substrate.

Acknowledgment. We thank the National Science Foundation (Grant CHE83-08064) and the Office of Naval Research for support of this research. We also thank the Johnson Matthey Co., Inc., for a generous loan of iridium salts. We are grateful to Amanda Kunin for preparation of the analytical sample of $\text{IrHBr}(\text{SiEt}_3)(\text{CO})(\text{dppe})$.

Registry No. **1a**, 98362-22-2; **1b**, 98362-23-3; **1c**, 98362-24-4; **1d**, 98362-25-5; **1e**, 98362-26-6; **2a**, 98462-82-9; **2b**, 98462-84-1; **2c**, 98462-86-3; **2d**, 98462-88-5; **3a**, 98462-83-0; **3b**, 98462-85-2; **3d**, 98462-89-6; **4c**, 98462-87-4; **5**, 98362-27-7; **6**, 98462-90-9; **7**, 98362-28-8; **8**, 98362-29-9; **9**, 98362-30-2; **10**, 98362-31-3; **11**, 98462-91-0; **I** ($\text{X} = \text{Br}$), 87985-33-9; **II** ($\text{X} = \text{Br}$), 88035-04-5; **III**, 87985-35-1; **IV**, 88035-06-7; $\text{IrBr}(\text{CO})(\text{dppe})$, 29638-05-9; $\text{Ir}(\text{CN})(\text{CO})(\text{dppe})$, 87985-30-6; $\text{IrI}(\text{CO})(\text{dppe})$, 85421-68-7; $\text{IrH}_2(\text{CN})(\text{CO})(\text{dppe})$, 98462-92-1; $\text{IrH}_3(\text{CO})(\text{dppe})$, 85421-67-6; Et_3SiH , 617-86-7; Ph_3SiH , 789-25-3; $(\text{EtO})_3\text{SiH}$, 998-30-1; Me_2ClSiH , 1066-35-9; MeCl_2SiH , 75-54-7; $\text{PPN}(\text{CN})$, 65300-07-4; **H1**, 10034-85-2; **HBr**, 10035-10-6; Et_3SiEt_3 , 1633-09-6; $\text{Et}_3\text{SiOSiEt}$, 994-49-0; Et_3SiBr , 1112-48-7.

Ferric Ion Sequestering Agents. 14.¹

1-Hydroxy-2(1H)-pyridinone Complexes: Properties and Structure of a Novel Fe-Fe Dimer

Robert C. Scarrow, David L. White,[†] and Kenneth N. Raymond*

Contribution from the Department of Chemistry, University of California, Berkeley, California 94720. Received December 26, 1984

Abstract: The 1-hydroxy-2-pyridonate (1,2-opo) ligating group has structural and electronic similarities to hydroxamate and catecholate ligands. A ligand with two 1,2-opo groups, 1,5-bis[(1,2-dihydro-1-hydroxy-2-oxopyridin-6-yl)carbonyl]-1,5-diazapentane (LH_2 , **5**), has been prepared and its properties have been compared with a dihydroxamate of microbial origin, rhodotorulic acid (H_2RA , **6**). Like RA , reaction of L^{2-} with Fe^{3+} in aqueous solution gives a dimeric complex, Fe_2L_3 . The structural and solution thermodynamic properties of this novel analogue of the siderophore RA have been investigated. One form of Fe_2L_3 crystallizes from dichloromethane-methanol-water to give orange-red hexagonal needles, $\text{Fe}_2\text{L}_3 \cdot 2\text{CH}_3\text{OH} \cdot \text{H}_2\text{O}$, space group $P6_1$ ($a = 13.731$ (2) Å, $c = 48.430$ (5) Å, $V = 7908$ (2) Å³ at -99 ± 3 °C, $d_{\text{obsd}} 1.53$ at 25 °C, $d_{\text{calcd}} 1.553$ at -99 °C). The structure is composed of six discrete Fe_2L_3 molecules in which each Fe^{3+} is surrounded by three bidentate opo groups such that the inner coordination sphere of both iron atoms and the entire molecule have pseudo- D_3 symmetry and a left-handed screw conformation (Δ -cis coordination about each iron atom). Since the ligand is achiral, the chirality of the crystal results from resolution during crystallization. This is the same geometry as that proposed for Fe_2RA_3 . Full-matrix least-squares refinement of the structure with 5077 reflections [$F_o^2 > 3\sigma(F_o^2)$] and 756 variable parameters converged with R and R_w indices of 0.0438 and 0.0489, respectively. The formation constant ($\log \beta_{230}$) for Fe_2L_3 is 52.3 (3) in aqueous solution, $\mu = 0.1$ M. The pK_a 's of H_2L were determined by potentiometric titration to be 5.35 (1) and 4.50 (1). Unlike hydroxamate siderophores, H_2L rapidly removes iron from the human serum iron protein transferrin: at 1.6 mM, H_2L removed iron from the protein (0.13 mM) in 0.1 M pH 7.4 tris buffer at 25 °C with a pseudo-first-order rate constant of $k_{\text{obsd}} = 1.08 \times 10^{-2} \text{ min}^{-1}$.

As reviewed recently,²⁻⁴ we have been engaged in the preparation of synthetic analogues of the siderophores, highly specific ferric chelating agents of microbial origin.⁵ Interest in these synthetic compounds includes their coordination chemistry as it relates to the siderophores^{2,6} but extends to their potential ap-

plication as clinical iron removal agents in man. Particularly in the disease β -thalassemia, where iron overload occurs as a side

(1) Previous paper in this series: Scarrow, R. C.; Riley, P. E.; Abu-Dari, K.; White, D. L.; Raymond, K. N. *Inorg. Chem.* 1985, 24, 954-67.

(2) Raymond, K. N.; Tufano, T. P. In "The Biological Chemistry of Iron"; Dunford, H. B., Dolfin, D., Raymond, K. N., Seiker, L., Eds.; D. Reidel Publishing Co.: Dordrecht, Holland, 1982; pp 85-105.

[†] Materials and Molecular Research Division, Lawrence Berkeley Laboratory.

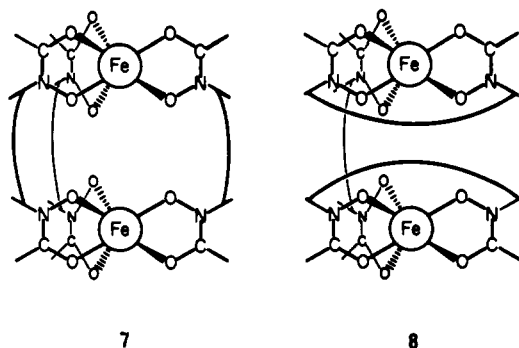
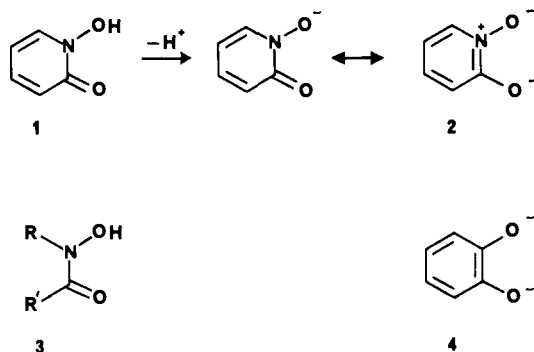


Figure 1. Two possible structures for ferric hydroxamate or 1-hydroxy-2(1H)-pyridinonate dimers. The arcs represent the connecting portions of the ligands; only the chelating portions of pyridonate rings are indicated. Structure 7 is that previously proposed for the ferric complex of rhodotorulic acid.^{14,15}

effect of periodic whole blood transfusion, an improved chelating agent is highly desirable.^{3,4} In a parallel effort, ligands highly specific for Pu(IV) and other actinide(IV) ions have been prepared, based on the strong chemical and biochemical similarities of Pu(IV) and Fe(III).^{7,8} In both programs initial efforts have been devoted largely to ligands incorporating catechol ligating groups, since the most powerful complexing agent for Fe(III), the siderophore enterobactin,² incorporates three catechol groups as a hexadentate ligand.

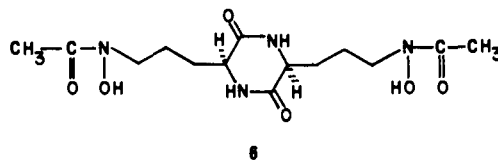
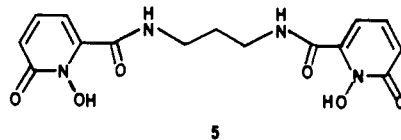
Transition-metal catechol complexes often are mononuclear with three bidentate catecholate ligands per metal, although other structural types are known.⁹ The weak acidity of catechol and the required loss of two protons per catechol group at neutral pH limit the effectiveness of catechol-based ligands at neutral pH or below.⁷ For this reason, we recently began a study of chelating hydroxypyridinone ligands ("HOPO's").^{1,7,10} Derivatives of 1-hydroxy-2(1H)-pyridinone (**1**) are of particular interest, since



its monoanion has a zwitterionic resonance form (**2**) that is isoelectronic with the catechol dianion (**4**). Alternatively, it can be viewed as a cyclic hydroxamic acid (cf. **1** and **3**). Since the metal-binding ligands in siderophores are usually either catechols

or hydroxamic acids, the 1,2-HOPO ligand **1** is an analogue of both common types of siderophore.

Among the first ligands that we prepared¹¹ was the 1,2-HOPO analogue of the catecholylic ligand 3-LICAM,¹² 1,5-bis[(1,2-dihydro-1-hydroxy-2-oxopyridin-6-yl)carbonyl]-1,5-diazapentane (**5**, "3-HOPOCAM-1,2"). This ligand also bears certain simi-



larities to rhodotorulic acid (**6**, "RA"), a dihydroxamate siderophore that has been isolated from low-iron cultures of *Rhodotorula pilimanae* and related yeasts.¹³ The tetradentate RA reacts with ferric ion at neutral pH to form the dimer $\text{Fe}_2(\text{RA})_3$, which was proposed to have the triply-bridged structure **7** shown in Figure 1.^{14,15} We have found that the diprotic, tetradentate 3-HOPOCAM-1,2 (H_2L) similarly reacts with ferric ion to yield a neutral, crystalline Fe_2L_3 complex. Its X-ray crystal structure has been determined, revealing a triply-bridged binuclear species analogous to that proposed for $\text{Fe}_2(\text{RA})_3$. In addition, this complex has been characterized by magnetic susceptibility, spectroscopy, and solution equilibrium measurements.

Like the catechol ligands, this prototypical multidentate HOPO chelating agent is kinetically competent in removing iron in vitro from the human serum iron transport protein transferrin (vide infra). Furthermore, it is an effective complexing agent for plutonium(IV), as determined by its in vivo efficacy in removing trace amounts of Pu from mice.¹⁶

Experimental Section

Infrared and UV-vis spectra were obtained with with Perkin-Elmer Model 283 and Hewlett-Packard Model 8450a spectrophotometers, respectively. The latter was equipped with a Model 8901A temperature controller. Magnetic susceptibility data were obtained on a SHE 905 SQUID magnetometer. Microanalyses were performed by the Microanalytical Laboratory, Chemistry Department, University of California, Berkeley.

Preparation of Fe_2L_3 ($\text{H}_2\text{L} = \mathbf{5}$). A solution of 155 mg (0.38 mmol) of $\text{Fe}(\text{NO}_3)_3 \cdot 9\text{H}_2\text{O}$ in 2 mL of water was added dropwise to a solution of 200 mg (0.57 mmol) of **5**¹¹ in 10 mL of water. A bright orange solid immediately precipitated, and the pH of the reaction mixture fell to 1.6. The pH was adjusted with 1 M KOH to 7, and the precipitate was isolated by filtration and washed with water. The moist precipitate was dissolved in 15 mL of 1:1 MeOH- CH_2Cl_2 , and this mixture was filtered to remove a trace of dark brown insoluble material. Evaporation of the filtrate and drying of the residue in vacuo at 25 °C gave 172 mg (78%) of amorphous orange product; IR (mineral oil mull) 1678 (s), 1609 cm^{-1} (s).

Recrystallization of Fe_2L_3 from dichloromethane gave elongated crystals with thin diamond-shaped cross sections. Solution NMR indicated the presence of dichloromethane, and the density (1.55 g/cm^3 in aqueous ZnCl_2) was consistent with the formulation $\text{C}_{45}\text{H}_{42}\text{N}_{12}\text{O}_{18} \cdot \text{Fe}_2 \cdot 3\text{CH}_2\text{Cl}_2$. Apparently some solvent was lost prior to analysis. Anal. C, H, N, Fe_2O_3 . Cl calcd 15.2; found 11.2.

Orange-red hexagonal needles were obtained by evaporating a solution of amorphous material in 1:1 MeOH- CH_2Cl_2 containing a small amount

(3) Martell, A. E.; Anderson, D. G.; Badman, D. G., Eds. "Development of Iron Chelators for Clinical Use"; Elsevier/North-Holland: Amsterdam, 1981.

(4) Raymond, K. N.; Harris, W. R.; Carrano, C. J.; Weilt, F. L. In "Inorganic Chemistry in Biology and Medicine"; Martell, A. E., Ed.; American Chemical Society: Washington, DC, 1980; ACS Symp. Ser. No. 140, pp 313-32.

(5) Raymond, K. N.; Müller, G.; Matzanke, B. F. In "Topics in Current Chemistry"; Boschke, F. L., Ed.; Springer-Verlag: Berlin, 1984; Vol. 123, pp 49-102.

(6) Matzanke, B. F.; Müller, G. I.; Raymond, K. N. *Biochem. Biophys. Res. Commun.* **1984**, *121*, 922-30.

(7) Raymond, K. N.; Freeman, G. E.; Kappel, M. J. *Inorg. Chim. Acta* **1984**, *94*, 193-204.

(8) Raymond, K. N.; Kappel, M. J.; Pecoraro, V. L.; Harris, W. J.; Carrano, C. J.; Weilt, F. L.; Durbin, P. W. In "Actinides in Perspective"; Edelstein, N. M., Ed.; Pergamon Press: Oxford and New York, 1982; pp 491-507.

(9) Pierpont, C. G.; Buchanan, R. M. *Coord. Chem. Rev.* **1981**, *38*, 45-87.

(10) Riley, P. E.; Abu-Dari, K.; Raymond, K. N. *Inorg. Chem.* **1983**, *22*, 3940-4.

(11) White, D. L.; Raymond, K. N., in preparation.

(12) Weilt, F. L.; Raymond, K. N. *J. Am. Chem. Soc.* **1980**, *102*, 2289-93.

(13) Atkin, C. L.; Neilands, J. B. *Biochemistry* **1968**, *7*, 3734-9.

(14) Carrano, C. J.; Raymond, K. N. *J. Am. Chem. Soc.* **1978**, *100*, 5371-4.

(15) Carrano, C. J.; Cooper, S. J.; Raymond, K. N. *J. Am. Chem. Soc.* **1979**, *101*, 599-604.

(16) Durbin, P. W.; White, D. L.; Raymond, K. N., in preparation.

(1–2%) of water. Anal. ($C_{48}H_{42}N_{12}Fe_2 \cdot 2CH_3OH \cdot H_2O$) C, H, N.

Crystallography. An Enraf-Nonius CAD4 diffractometer equipped with a universal low-temperature device, a PDP 11/60 computer, and SDP software¹⁷ locally modified by Dr. F. Hollander were used. Details of data collection and refinement methods are given elsewhere.¹⁸ In this study monochromated Cu K α radiation ($\lambda = 1.5418 \text{ \AA}$) was used because of the large unit cells involved for both crystal forms isolated.

Precession photography and diffractometry were used to establish the space group of the CH_2Cl_2 -solvated crystals as $P2_1/c$ with room-temperature dimensions $a = 22.203(4) \text{ \AA}$, $b = 13.125(2) \text{ \AA}$, $c = 42.06(4) \text{ \AA}$, $\beta = 79.70(4)^\circ$, and $V = 12059(12) \text{ \AA}^3$. The large cell volume indicates eight Fe_2L_3 units per unit cell. Because of the large asymmetric unit, the structure of the monoclinic crystals was not pursued.

Precession photography of the hexagonal crystals indicated the space group to be either $P6_1$ or $P6_5$. The hexagonal needles visibly fractured several hours after being removed from solvent (density measurements suggest this is due to loss of one methanol of solvation). Thus after cleavage normal to the c axis to give a $\sim 0.2\text{-mm}^3$ fragment, the data crystal was mounted in a thin-walled quartz capillary and maintained at $-99 \pm 3 \text{ }^\circ\text{C}$ [$a = 13.731(2) \text{ \AA}$, $c = 48.430(5) \text{ \AA}$, $V = 7908(2) \text{ \AA}^3$, and $Z = 6$]. The 7775 unique observed data were empirically corrected for absorption,¹⁸ rotation around the diffraction vector gave at most a 29% variation in intensity.

Potentiometric Titration. A 2.1 mM solution of **5** was titrated under argon with standardized 0.1 M KOH containing 0.5% carbonate. The procedure for calibrating the TRIZMA (Sigma) electrode and Brinkmann 102 pH meter has been reported previously.¹ The pK_a 's of the ligand were computer fit to the data.¹⁹ Ionic strength of 0.1 M was maintained with $NaClO_4$.

EDTA Competition. Buffered solutions ($[OAc^-] = 0.010 \text{ M}$, $[KNO_3] = 0.090 \text{ M}$, and $[HOAc] = 0.010$ or 0.002) containing Fe^{3+} , **5**, and EDTA were maintained in 10-cm UV cells at $25.0 \text{ }^\circ\text{C}$ using a Brinkmann Lauda K-2/R water bath. Nine to twelve hours was allowed for equilibration; this was sufficient as judged by identity of spectra of solutions approaching the same equilibrium from different directions. The observed spectra allowed computation of the Fe_2L_3 formation constant.¹

Iron Removal from Transferrin. Human serum transferrin (98%, Sigma) was used as supplied. An approximately 0.2 mM solution was prepared in pH 7.4, 0.1 M Tris chloride buffer with 0.05 M $KHCO_3$ added, and the true concentration was determined by monitoring Abs_{460nm} as 1:3 iron(III)/NTA solution (0.0111 M Fe^{3+} , pH 6.7) was added.²⁰ The titration sample was recombined with the rest of the original apo-transferrin solution and the correct amount of Fe/NTA solution was added to give $Fe_{2.00}Tf$. This solution was passed down a 42 cm \times 2.5 cm i.d. column of pre-equilibrated Sephadex G-25 (Pharmacia, particle size 20–80 μm) and eluted with 0.10 M $NaClO_4$. The orange band was collected, rotary evaporated to near dryness (Caution! Organic perchlorate), redissolved in ca. 1 mL of water, and passed down the Sephadex column, this time equilibrated and eluted with the 0.10 M Tris chloride buffer (pH 7.4 at $25 \text{ }^\circ\text{C}$) used in the subsequent kinetics study. All but the trailing edge (10%) of the orange band was collected and used as a Fe_2Tf stock solution for the subsequent experiments. The concentration was estimated spectrophotometrically. The iron removal kinetics and concentration were determined spectrophotometrically at $25 \text{ }^\circ\text{C}$, with the solutions in contact with air.

Results

Crystallography. The structure was solved by standard heavy-atom methods, assuming space group $P6_1$. The least-squares refinement was on $|F|$ and used the 5077 independent reflections with $I > 3\sigma(I)$. A p factor of 0.04¹⁸ was used to calculate $\sigma(F^2)$. The water and one methanol were clearly evident in the difference Fourier maps. The site assigned to the second methanol is severely disordered; several structural models were evaluated based on their ability to describe the electron density and to reduce the computed residuals. The model chosen has two quarter-occupancy methanols that share a carbon atom position, and a separate half-occupancy methanol. The distinction between oxygen and carbon atoms was based on the plausibility of hydrogen bonding.

Positions of all non-hydrogen atoms and their anisotropic thermal parameters (except for the quarter-occupancy oxygens)

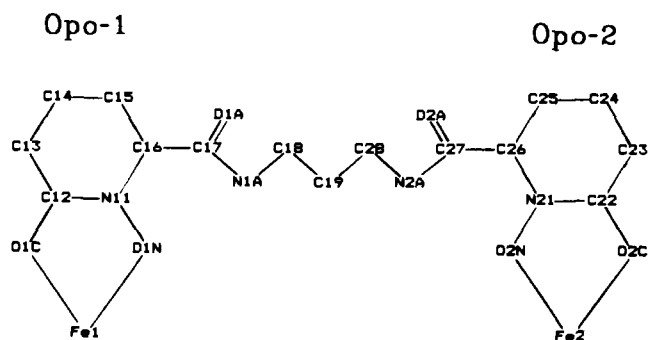


Figure 2. Atom-naming scheme for one ligand of Fe_2L_3 . The other ligands are named by adding 2 and 4 (respectively) to the first digit of the name. Thus opo-3 and opo-4 lie on the same ligand, as do opo-5 and opo-6. OW and CM-OM are the full-occupancy water and methanol, CM1-OM1 is the half-occupancy methanol, and CM2-OM2 and CM2-OM3 are the two quarter-occupancy methanols.

Table I. Crystallographic Summary for Hexagonal Crystals of $Fe_2(C_{15}H_{14}N_4O_6)_3 \cdot H_2O \cdot 2CH_3OH$ ($C_{47}H_{52}Fe_2N_{12}O_{21}$)

formula weight	1232.7
space group	$P6_1$
a , \AA	13.731 (2) ^a
c , \AA	48.430 (5)
volume, \AA^3	7908 (2)
z , formula units/cell	6
calcd density, g/cm^3	1.553
obsd density, g/cm^3	1.51–1.55 ^b
Cu K α wavelength, \AA	1.5418
range of 2θ , deg	2–120
unique reflections measd, not systematically absent	7775
obsd reflections ^c (n_o)	5077
refined parameters (n_v)	756
extinction parameter (refined)	$2.0(1) \times 10^{-7}$
R^d	0.044
R_w^d	0.049
R_{all}^d	0.110
GOF ^d	1.40
largest $e/\text{\AA}^3$ in final difference Fourier	0.47

^a The esd's of the last digit are shown in parentheses. Cell constants were determined from the refinement of the setting angles for 24 high-angle reflections. The temperature was $-99 \pm 3 \text{ }^\circ\text{C}$. ^b Three density determinations by flotation were performed. In aqueous $ZnCl_2$ a value of 1.53 g/cm^3 was obtained. Crystals exposed to air for several months gave $D = 1.51 \text{ g/cm}^3$ (aqueous CsCl), suggesting loss of one methanol per formula unit. The same crystals left overnight in 1:2 MeOH/ H_2O (+CsCl) had $D = 1.55 \text{ g/cm}^3$. ^c Reflections with $F^2 > 3\sigma(F^2)$ were considered observed and used in the least-squares refinement. ^d Error indices are defined as follows: $R = (\sum ||F_o| - |F_c||) / \sum |F_o|$, $R_w = [(\sum w(|F_o| - |F_c|)^2) / \sum wF_o^2]^{1/2}$, and $GOF = [(\sum w(|F_o| - |F_c|)^2) / (n_o - n_v)]^{1/2}$, where F_o and F_c are observed and calculated structure factors, the weight $w = 4F^2/\sigma^2(F^2)$, and the sum is over all observed reflections. ^e R_{all} is defined as is R except the sum is over all measured reflections.

were refined by full-matrix least-squares methods. All full-occupancy hydrogen atoms were located in difference Fourier maps and placed in the structure model as isotropic atoms ($B_{iso} = 5.0 \text{ \AA}^2$, except for the methanol) at idealized positions 0.95 \AA from the bonded atom. Late in the refinement the structure was inverted to $P6_5$ and refined further. This gave R and R_w values approximately triple those obtained with $P6_1$. This confirmed the initial choice of space group.

The final refinement of this large structure was of 756 parameters, including scale and secondary extinction [$2.0(1) \times 10^{-7}$] parameters. Computed residuals¹⁸ were $R = 0.044$ and $R_w = 0.049$, and $GOF = 1.40$. The largest peaks in the final difference Fourier ($0.47 e/\text{\AA}^3$), the largest shift/esd ratio (1.5 in a thermal parameter), and the highest correlation coefficients (not symmetry imposed) all involved the disordered methanol. Refined positional parameters and isotropic equivalent thermal parameters are given in Table II. Atom naming is explained in Figure 2. Anisotropic thermal parameters, hydrogen atom positions, and observed and

(17) "Structure Determination Package User's Guide"; B. A. Frenz and Associates, Inc.: College Station, TX, 1982.

(18) Eigenbrot, C. W., Jr.; Raymond, K. N. *Inorg. Chem.* **1982**, *21*, 2653–60.

(19) Motekaitis, R. J.; Martell, A. E. *Can. J. Chem.* **1982**, *60*, 168.

(20) Bates, G. W.; Schlabach, N. R. *J. Biol. Chem.* **1973**, *248*, 3228–32.

Table II. Refined Positions and Equivalent Isotropic Thermal Parameters for Non-Hydrogen Atoms of Fe₂(C₁₅H₁₄N₄O₆)₃·H₂O·CH₃OH^a

atom	x	y	z	B, Å ²	atom	x	y	z	B, Å ²
Fe1	0.48757 (6)	0.50084 (7)	0.000	2.83 (2)	C25	0.1580 (6)	0.4243 (6)	0.0909 (2)	4.9 (2)
Fe2	0.27509 (6)	0.92792 (7)	-0.00267 (2)	2.24 (2)	C26	0.2476 (5)	0.7766 (5)	0.0727 (1)	3.5 (2)
O1N	0.5984 (3)	0.6651 (3)	0.00521 (9)	3.2 (1)	C27	0.3569 (5)	0.7851 (5)	0.0811 (1)	3.3 (2)
O1C	0.6318 (3)	0.5047 (3)	-0.0063 (1)	3.3 (1)	C28	0.5331 (5)	0.7963 (6)	0.0675 (2)	4.4 (2)
O1A	0.8623 (4)	0.9777 (4)	0.0242 (1)	7.8 (2)	C32	0.3992 (5)	0.4644 (5)	0.0534 (1)	3.0 (2)
O2N	0.3161 (3)	0.8660 (3)	0.03011 (8)	2.3 (1)	C33	0.3770 (5)	0.4439 (5)	0.0819 (2)	4.2 (2)
O2C	0.1465 (3)	0.8866 (3)	0.02216 (9)	3.3 (1)	C34	0.2897 (6)	0.4486 (6)	0.0930 (1)	4.3 (2)
O2A	0.3760 (4)	0.7858 (4)	0.10578 (9)	5.8 (2)	C35	0.2198 (5)	0.4738 (5)	0.0775 (1)	3.2 (2)
O3N	0.3562 (3)	0.5178 (3)	0.01185 (8)	2.6 (1)	C36	0.2419 (4)	0.4965 (5)	0.0504 (1)	2.6 (2)
O3C	0.4762 (3)	0.4597 (3)	0.04015 (9)	3.4 (1)	C37	0.1687 (4)	0.5180 (4)	0.0306 (1)	2.1 (1)
O3A	0.1992 (3)	0.6119 (3)	0.02210 (8)	2.8 (1)	C38	-0.0076 (5)	0.2448 (5)	0.0051 (1)	3.3 (2)
O4N	0.2066 (3)	0.7864 (3)	-0.02519 (8)	2.7 (1)	C39	0.0069 (5)	0.3888 (5)	-0.0235 (1)	3.1 (2)
O4C	0.2080 (3)	0.9697 (3)	-0.03365 (8)	3.1 (1)	C42	0.1740 (4)	0.9007 (5)	-0.0544 (1)	3.1 (2)
O4A	0.1051 (4)	0.5447 (3)	-0.0867 (1)	5.2 (1)	C43	0.1414 (6)	0.9210 (5)	-0.0802 (2)	4.7 (2)
O5N	0.4591 (3)	0.5390 (3)	-0.03773 (9)	2.9 (1)	C44	0.1046 (6)	0.8394 (6)	-0.0998 (2)	5.3 (2)
O5C	0.3938 (3)	0.3480 (3)	-0.01511 (9)	3.2 (1)	C45	0.1023 (5)	0.7387 (5)	-0.0949 (1)	4.0 (2)
O5A	0.3381 (4)	0.5751 (4)	-0.1143 (1)	6.2 (2)	C46	0.1355 (5)	0.7186 (5)	-0.0701 (1)	2.8 (2)
O6N	0.4230 (3)	0.9639 (3)	-0.01931 (8)	2.13 (9)	C47	0.1278 (5)	0.6060 (5)	-0.0664 (1)	3.0 (2)
O6C	0.3676 (3)	1.0885 (3)	0.00714 (8)	2.4 (1)	C48	0.1216 (4)	0.4623 (5)	-0.0360 (1)	2.6 (2)
O6A	0.7467 (3)	1.0894 (3)	-0.0484 (1)	5.5 (1)	C52	0.3449 (4)	0.3438 (4)	-0.0378 (2)	3.5 (2)
N1A	0.6768 (4)	0.8781 (4)	0.0170 (1)	3.2 (1)	C53	0.2595 (5)	0.2478 (5)	-0.0510 (2)	4.0 (2)
N2A	0.4245 (4)	0.7853 (4)	0.0613 (1)	3.6 (1)	C54	0.2161 (6)	0.2576 (6)	-0.0749 (2)	4.8 (2)
N3A	0.0731 (3)	0.4251 (4)	0.0249 (1)	2.5 (1)	C55	0.2570 (5)	0.3615 (5)	-0.0877 (1)	4.3 (2)
N4A	0.1417 (4)	0.5754 (4)	-0.0411 (1)	2.7 (1)	C56	0.3362 (5)	0.4562 (5)	-0.0757 (1)	3.3 (2)
N5A	0.3939 (4)	0.6546 (4)	-0.0728 (1)	3.7 (1)	C57	0.3792 (5)	0.5702 (5)	-0.0595 (1)	4.1 (2)
N6A	0.5829 (3)	0.9301 (4)	-0.0405 (1)	3.0 (1)	C58	0.4323 (5)	0.7645 (5)	-0.0844 (1)	3.9 (2)
N11	0.7079 (4)	0.6910 (4)	0.0017 (1)	2.9 (1)	C59	0.5588 (5)	0.8363 (5)	-0.0854 (1)	3.8 (2)
N21	0.2344 (4)	0.8224 (4)	0.0493 (1)	2.8 (1)	C62	0.4728 (4)	1.1332 (4)	0.0016 (1)	2.4 (1)
N31	0.3325 (4)	0.4949 (4)	0.0392 (1)	2.4 (1)	C60	0.5550 (5)	1.2447 (4)	0.0082 (1)	3.1 (2)
N41	0.1716 (3)	0.8011 (3)	-0.0505 (1)	2.4 (1)	C64	0.6637 (5)	0.2841 (5)	0.0004 (2)	4.1 (2)
N51	0.3765 (4)	0.4447 (3)	-0.0508 (1)	3.1 (1)	C65	0.6926 (5)	1.2169 (5)	-0.0145 (1)	3.2 (2)
N61	0.5064 (3)	1.0698 (3)	-0.0128 (1)	2.1 (1)	C66	0.6156 (4)	1.1094 (4)	-0.0208 (1)	2.7 (2)
C12	0.7208 (4)	0.6011 (5)	-0.0045 (1)	3.0 (2)	C67	0.6506 (5)	1.0394 (4)	-0.0379 (1)	3.1 (2)
C13	0.8316 (5)	0.6250 (5)	-0.0100 (2)	4.1 (2)	C68	0.6111 (5)	0.8574 (5)	-0.0563 (2)	3.8 (2)
C14	0.9183 (5)	0.7290 (5)	-0.0071 (2)	4.4 (2)	OW	0.4123 (3)	0.4345 (3)	-0.00795 (9)	3.9 (1)
C15	0.9010 (5)	0.8174 (5)	0.0007 (2)	4.3 (2)	OM	0.0389 (4)	0.1965 (4)	0.0294 (1)	6.0 (2)
C16	0.7938 (4)	0.7967 (5)	0.0053 (1)	3.3 (2)	CM	0.1217 (7)	0.2005 (7)	0.0132 (2)	7.5 (3)
C17	0.7786 (5)	0.8914 (5)	0.0160 (2)	4.1 (2)	OM1(1/2)	0.9430 (9)	1.085 (1)	-0.0432 (4)	12.0 (5)
C18	0.6480 (5)	0.9518 (5)	0.0335 (2)	4.0 (2)	OM2(1/4)	0.837 (2)	1.005 (2)	-0.0911 (5)	8.7 (7) ^b
C19	0.6290 (5)	0.9159 (2)	0.0634 (1)	3.7 (2)	OM3(1/4)	0.941 (2)	1.003 (2)	0.0869 (6)	9.5 (9) ^b
C22	0.1405 (5)	0.8296 (5)	0.0441 (1)	3.4 (2)	CM1(1/2)	0.947 (1)	1.004 (1)	-0.0536 (5)	9.0 (6)
C23	0.0517 (5)	0.7791 (7)	0.0629 (2)	5.5 (2)	CM2(1/2)	0.918 (1)	1.034 (2)	-0.0703 (4)	10.0 (6)
C24	0.0604 (6)	0.7253 (7)	0.0851 (2)	5.9 (3)					

^aEds's of the last digit are shown in parentheses. Figure 2 shows the atom-naming scheme. The last five entries in the table account for the disordered methanol (occupancies in parentheses). ^bAtoms were refined with isotropic thermal parameters.

calculated structure factors are given in Tables S1, S2, and S3,²¹ respectively. Bond lengths and angles are shown in Table S4.²¹

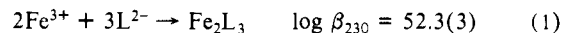
Magnetic Susceptibility. Magnetic susceptibility measurements were carried out on hexagonal crystals that had been removed from solvent for several months. Density data and weight loss at 110 °C in vacuo indicated that only one methanol and one water of solvation remained. This was taken into account in calculating χ_m and χ_{diam} . The data followed Curie law behavior throughout the temperature range studied (5–300 K). The average μ_{eff} was 5.681 (5) μ_B , per iron atom. The magnetic susceptibility was also determined in 9:1 (v/v) CDCl₃-CD₃OD at 301 K by the NMR method.²² Under these conditions, the μ_{eff} per iron atom was the same, 5.7 μ_B .

UV-vis Spectra. In pH 7.4, 0.1 M Tris buffer, **5** has spectral features at 221 ($\epsilon = 3.0 \times 10^4 \text{ cm}^{-1} \text{ M}^{-1}$), 238 (3.4×10^4), and 344 (1.0×10^4) nm. Upon the addition of ferrous ammonium sulfate solution, the characteristic orange color of the ferric complex appears, and the color change is complete within a few minutes. After the addition of 0.67 equiv of iron, the ligand-based UV bands are blue-shifted to 218 ($\epsilon = 3.9 \times 10^4 \text{ cm}^{-1} \text{ M}^{-1}$ per ligand) and 306 (1.0×10^4) nm, and a barely defined peak on the edge of the ligand-based absorbance at 400 nm ($\epsilon = 4000$ per Fe) appears. As additional Fe³⁺ is added, the UV spectrum changes only slightly, but the peak in the visible spectrum changes

to a shoulder. This is apparently due to a slight blue shift that occurs with little change in intensity (the minimum in the second-derivative spectrum moved from 448 to 435 nm). Once an excess of iron is present, however, the solution rapidly becomes turbid, presumably due to formation of hydrated ferric oxide colloid.

Job's plot of absorbance at 400 and 450 nm in pH 5.25 acetate buffer showed a maximum absorbance for a 3:2 ligand:metal ratio.

Solution Equilibria. The pK_a's of **5**, as determined by potentiometric titration, are 5.35 (1) and 4.50 (1). From spectra of solutions in which EDTA competed with **5** for Fe(III), the pK_a's of the ligands and the formation constant of FeEDTA⁻,²³ it is possible to determine the formation constant for eq 1. The value



shown represents the average of five values determined at pH 4.55 ($C_{Fe} = 0.015 \text{ mM}$, $C_L = 0.030 \text{ mM}$, $C_{EDTA} = 0.20\text{--}1.56 \text{ mM}$) and one value determined at pH 5.23 ($C_{Fe} = 0.019 \text{ mM}$, $C_L = 0.022 \text{ mM}$, $C_{EDTA} = 0.39 \text{ mM}$). The indicated standard deviation largely reflects uncertainty in the formation constant of FeEDTA⁻; the standard deviation of the competition constant is only 0.1 log unit.

Kinetics of Iron Removal from Transferrin. The isobestic spectral changes from addition of **5** (1.6 mM) to diferic transferrin in pH 7.4 Tris buffer are shown in Figure 3. The inset shows

(21) Tables S1–S4 (53 pages) are supplementary material. Ordering information is given on any current masthead page.
(22) Evans, D. F. J. *Chem. Soc.* **1959**, 2003–5.

(23) Smith, R. M.; Martell, A. E. "Critical Stability Constants"; Plenum Press: New York, 1976; Vol. 3.

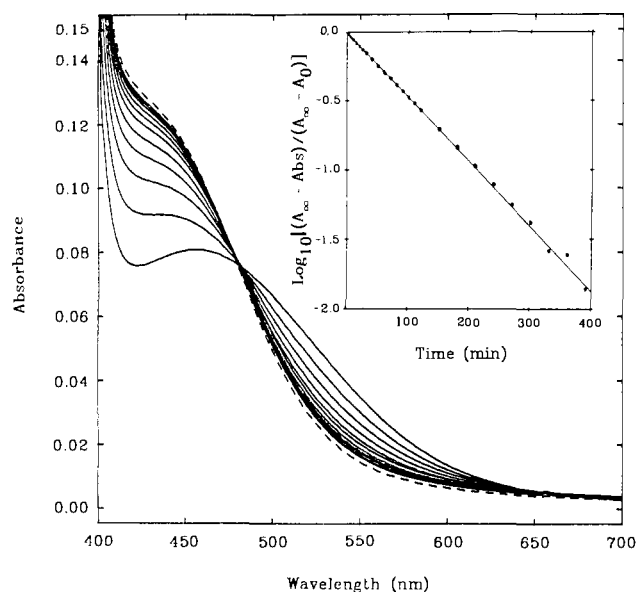


Figure 3. Absorbance changes with time after **5** (1.6 mM) was added to diferric transferrin (0.013 mM) in pH 7.4, 0.1 M Tris (Cl⁻) buffer. Spectra were taken at 30 s after mixing, every 30 min to 300 min, and then at 510 min (dashed curve), which was used for A_{∞} . The inset demonstrates the pseudo-first-order kinetics. The absorbance illustrated is $\text{av}(\text{Abs}(410\text{--}430\text{ nm})) - \text{av}(\text{Abs}(750\text{--}800\text{ nm}))$, with the latter term included to eliminate small base line fluctuations.¹

a plot of $\log [(A_{\infty} - \text{Abs})/(A_{\infty} - A_0)]$ as a function of time. From the slope of this graph one obtains a pseudo-first-order $k_{\text{obsd}} = 1.08 \times 10^{-2} \text{ min}^{-1}$. After 30 min, 29% of the iron is removed; in contrast, only $2.0 \pm 0.4\%$ of the iron is removed when $[\mathbf{5}] = 0.20 \text{ mM}$, consistent with a first-order dependence of the rate of removal on the ligand at low concentration.

Discussion

3-HOPOCAM-1,2 as a Model of RA. The dihydroxamate diketopiperazine RA **6** is tetradentate and thus unable to satisfy the preferred octahedral coordination geometry of Fe(III) in a simple 1:1 complex. It was determined in earlier studies^{14,15} that (a) at neutral pH RA forms a binuclear complex with ferric ion, $\text{Fe}_2(\text{RA})_3$, (b) the ferric ions are each octahedrally coordinated to the hydroxamates of three RA's, and (c) the absolute configuration about each ferric ion is Δ -cis. Although no crystals of $\text{Fe}_2(\text{RA})_3$ have been obtained, spectral and molecular weight data led to the proposal of the triply-bridged structure **7** over the alternative structure **8** with a single bridging ligand (Figure 1).

We^{24,25} have prepared a number of linear dihydroxamate analogues of RA, and one of these formed a methoxide-bridged $\text{Fe}_2\text{L}_2(\text{OMe})_2$ complex, whose crystal structure has been determined.²⁵ Although this complex with its two bridging dihydroxamate ligands lent support for the formulation of $\text{Fe}_2(\text{RA})_3$ as a triply-bridged species, similar ligands differing by only one methylene unit in backbone length failed to give similar crystalline bridged species.

The ligand 3-HOPOCAM-1,2 is similar to RA in several important respects. As noted earlier, the 1-hydroxy-2(1*H*)-pyridinone functionality can be thought of as a cyclic hydroxamic acid, and bond lengths obtained by X-ray crystallography of HOPO derivatives^{1,10} support this representation. Both this ligand and RA are dianionic and tetradentate. Molecular models indicate that the distances between the hydroxamates in the extended molecules are approximately the same, ca. 12 Å. Thus 3-HOPOCAM-1,2 can serve as a useful model of RA. The demonstration that it forms a triply-bridged Fe_2L_3 complex with Δ -cis octahedral coordination about the Fe atoms lends strong support to the

Table III. Comparison of Bond Lengths (Å) Determined in Disordered $\text{Fe}(1,2\text{-opo})_3$ with Corresponding Average Distances in $\text{Fe}_2(\text{C}_{15}\text{H}_{14}\text{N}_4\text{O}_6)_3$ ^a

bond(s)	$\text{Fe}(1,2\text{-opo})_3$ ^b	Fe_2L_3 ^c
Fe-O1, Fe-O2	2.008 (1)	1.994 (10) ^d
O1-N1, O2-C2	1.320 (2)	1.324 (6)
N1-C2	1.364 (2)	1.368 (7)
N1-C6, C2-C3	1.377 (2)	1.384 (6)
C5-C6, C3-C4	1.356 (2)	1.354 (9)
C4-C5	1.400 (3)	1.387 (10)

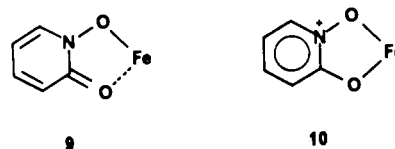
^aThe numbering scheme is analogous to that of Figure 2, but with the first digit removed. ^bReference 1. Esd's of the last decimal place are given in parentheses. ^cThis work. Average values from all six half-ligands are given. The variance over the six half-ligands is indicated in parentheses. ^dIf opo-3 (see Figure 2) is excluded, the average Fe-O bond length over the other five ligands is 1.991 (5) Å.

analogous formulation (**7**) for $\text{Fe}_2(\text{RA})_3$. Indeed, some synthetic mono- and dihydroxamates and monomeric 1-hydroxy-2(1*H*)-pyridinones have been shown²⁶ to mediate iron uptake in *Rhodotorula pilulinae*, an RA-producing organism.

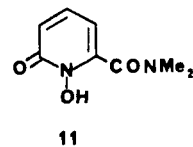
Crystallography. The structure of the hexagonal crystal of Fe_2L_3 consists of discrete molecules that, together with two methanols and one water of solvation, comprise the asymmetric unit. The inner coordination sphere of both iron atoms and the entire molecule have pseudo- D_3 symmetry and a left-handed screw conformation (Δ -cis coordination of the iron atoms); this is illustrated by the view in Figure 4 down the Fe-Fe axis. The view in Figure 5 is perpendicular to this axis. Since the free ligand is achiral, the chirality of the complex is due to a spontaneous resolution of individual crystals as they form.

The crystal structure would indicate no significant interaction between the two iron centers. The intramolecular Fe1-Fe2 distance is 7.75 Å; the closest iron-iron distance is *intermolecular* (6.89 Å). Average values for bond lengths and angles are shown in Figure 6. The bond lengths in the present structure are compared in Table III to those of the iron monomer tris(1-hydroxy-2-pyridinonato)iron [$\text{Fe}(1,2\text{-opo})_3$], which was found to be disordered by a symmetry-imposed twofold rotation axis that bisects the N1-C2 and C4-C5 bonds.¹ The determined bond lengths in $\text{Fe}(1,2\text{-opo})_3$ were postulated to represent averages of the two symmetry-related bonds. The average distances in Fe_2L_3 generally agree within error with those of $\text{Fe}(1,2\text{-opo})_3$, with the exception of the Fe-O distance (see below).

Two plausible resonance forms for the metalloxyypyridonate complex are shown in **9** and **10**: **9** shows the cyclic hydroxamate character, while **10** is a catechol-like resonance form. The in-



fluence of **9** is seen in the alternating (long-short) bond lengths, which agree within standard deviations with those found in an analogous free ligand, *N,N*-dimethyl-1,2-dihydro-1-hydroxy-2-oxypyridine-6-carboxamide (**11**).¹ However, neither compound



shows complete single-double bond alteration. The C-O bond distance of 1.28 Å is 0.04 Å longer than that found in **11** but is identical with the C-O distance in tris(benzohydroxamato)iron²⁷ and much shorter than the average 1.35-Å distance found in

(24) Smith, W. L.; Raymond, K. N. *J. Am. Chem. Soc.* **1980**, *102*, 1252-5.

(25) Barclay, S. J.; Riley, P. E.; Raymond, K. N. *J. Am. Chem. Soc.* **1982**, *104*, 6802-4.

(26) Müller, G.; Barclay, S. J.; Raymond, K. N. *J. Biol. Chem.*, in press.

(27) Linder, J. J.; Goettlicher, S. *Acta Crystallogr., Sect. B: Struct. Crystallogr. Cryst. Chem.* **1969**, *B25*, 832-42.

indicating only a weak interaction between the two ends of the ligand. The $\log \beta$ (and hence ΔG°) for the Fe_2L_3 complex of **5** is only slightly greater than twice that of the FeL_3 complex of **11** ($\log \beta = 25.6$).¹ In order to account for the effect of proton competition in ligand strength comparisons, we rank the relative iron-binding ability of ligand by the pM value, defined as $-\log [\text{Fe}^{3+}]$ of a pH 7.4 solution that is 10^{-5} M in total ligand and 10^{-6} M in total iron. The pM for **5** is 21.7, almost the same as the value of 21.9 for rhodotorulic acid (**6**), although 4–14 units less than the pM for siderophores containing *three* bidentate catechol or hydroxamate groups.⁵ The corresponding pM for transferrin is 23.6² (assuming $[\text{HCO}_3^-] = 0.024$ M), so that neither **5** nor **6** is expected to be (thermodynamically) effective of *in vivo* iron removal from transferrin at low (10 μM) concentrations. At higher concentrations of ligand, the equilibrium will shift to favor the Fe_2L_3 species, and indeed, **5** removes iron from transferrin at approximately millimolar concentrations. The rate of removal by 0.2 mM ligand is somewhat slower for **5** than for the tricatecholate ligands enterobactin, MECAM, and 3,4-LICAMS. These four ligands remove 2%, 6%, 10%, and 6%, respectively, of the iron from transferrin in 30 min.³³ At 1.6 mM the rate of removal by **5** is nearly the same as the rate interpolated for the sulfonated synthetic tricatechol ligand 3,4-LICAMS.³³ Thus at millimolar concentrations, **5** is a viable agent for iron removal from transferrin. Ligands incorporating three hydroxypyridinone

groups should be equally effective at removing iron from transferrin at even lower concentration.

Conclusions

The diprotic, tetradentate ligand 1,5-bis[(1,2-dihydro-1-hydroxy-2-oxopyridin-6-yl)carbonyl]-1,5-diazapentane (**5**) reacts with ferric ion to form a Fe_2L_3 complex. In the solid state this complex has the triply-bridged structure **7**, (Figure 1). The iron-complexing ability of **5** at neutral pH resembles that of the dihydroxamate siderophore rhodotorulic acid (**6**). Unlike rhodotorulic acid or other hydroxamate ligands (including desferrioxamine B, the current therapeutic agent for human iron overload), **5** is kinetically competent to remove iron from transferrin *in vitro* at millimolar concentrations.

Acknowledgment. We thank Dr. Fred Hollander of the U.C. Berkeley CHEXRAY Diffraction Facility (supported in part by the National Science Foundation) for his assistance with various technical aspects of the X-ray diffraction work. An NSF graduate fellowship to R.C.S. is gratefully acknowledged. This work was supported by NIH Grant AM-32999.

Registry No. **5**, 97570-39-3; $\text{Fe}_2(\text{C}_{15}\text{H}_{14}\text{N}_4\text{O}_6)_3 \cdot \text{H}_2\text{O} \cdot 2\text{CH}_3\text{OH}$, 97570-38-2; Fe, 7439-89-6.

Supplementary Material Available: Tables S1–S4, containing anisotropic thermal parameters, hydrogen atom positions, observed and calculated structure factors, and bond lengths and angles (53 pages). Ordering information is given on any current masthead page.

(33) Carrano, C. J.; Raymond, K. N. *J. Am. Chem. Soc.* **1979**, *101*, 5401–4.

Pericyclines of Order [5], [6], [7], and [8]. Simple Convergent Syntheses and Chemical Reactions of the First Homoconjugated Cyclic Polyacetylenes¹

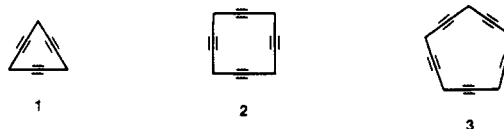
Lawrence T. Scott,* Gary J. DeCicco, James L. Hyun, and Gerd Reinhardt

Contribution from the Department of Chemistry and Center for Advanced Study, College of Arts and Science, University of Nevada, Reno, Nevada 89557. Received December 6, 1984. Revised Manuscript Received June 4, 1985

Abstract: Convergent syntheses are reported for the fully methylated derivatives of [5]-, [6]-, [7]-, and [8]pericycline (**23**, **26**, **29**, and **32**). All the carbon atoms in each of these homoconjugated cyclic polyacetylenes were derived from the same five-carbon starting material, 2-methyl-3-butyn-2-ol. An octamethyl derivative of [5]pericycline with a CH_2 group at one corner has also been prepared (**36**); however, attempts to synthesize derivatives of [3]- and [4]pericycline were not successful. A cyclic oligomerization approach to the synthesis of pericyclines unexpectedly gave octamethylcyclododeca-1,3,7,9-tetraene (**39**), an isomer of octamethyl[4]pericycline which also has four acetylenes in a 12-membered ring. Physical and spectroscopic properties of these new cyclic polyacetylenes are discussed. Decamethyl[5]pericycline (**23**) forms an isolable complex with silver triflate and reacts with $\text{Co}_2(\text{CO})_8$ to give both mono- and bis- $\text{Co}_2(\text{CO})_6$ complexes. The latter is formed with surprisingly high chemoselectivity. Similar chemistry is seen with dodecamethyl[6]pericycline (**26**). The free pericyclines can be recovered from their silver complexes by treatment with aqueous ammonia and from their cobalt complexes by oxidation with Ce(IV). Various other chemical reactions of these unusual new compounds are also reported.

Rings of atoms containing one or more $-\text{C}\equiv\text{C}-$ units ("cyclines") have aroused the curiosity of organic chemists for many years;^{2,3} however, surprisingly little attention has been accorded those rings comprised entirely of $-\text{C}\equiv\text{C}-$ units and

CH_2 groups joined together in alternation around the perimeter, e.g., **1**, **2**, and **3**. For this intriguing class of molecules, we have



suggested the name "pericyclines", an appellation which connotes the presence of alkyne functionality on every side of the ring.⁴

(1) Part 4 in the series on "Cyclines". For part 3, see ref 4; for part 5, see ref 27.

(2) Meier, H. *Synthesis* **1972**, 235–253.

(3) Nakagawa, M. In "The Chemistry of the Carbon–Carbon Triple Bond"; Patai, S., Ed.; Wiley-Interscience: New York, 1978; Vol. 2, pp 635–712.